Stepwise Assembly of Unsymmetrical Supramolecular Arrays Containing Porphyrins and Coordination Compounds

Enzo Alessio,*,† Enrica Ciani,† Elisabetta Iengo,† Vadim Yu. Kukushkin,†,‡ and Luigi G. Marzilli§

Dipartimento di Scienze Chimiche, Università di Trieste, 34127 Trieste, Italy, and Department of Chemistry, Emory University, Atlanta, Georgia 30322

Received June 17, 1999

The stepwise coordination of *meso*-4′-pyridyl/phenyl porphyrins (4′-PyPs) to different metal centers proved to be an efficient synthetic approach leading to unsymmetrical arrays containing porphyrins and coordination compounds. The first step of this process, treatment of 4′-PyPs with a less than stoichiometric amount of *cis*,*fac*-$RuCl_2(Me_2SO)_3(CO)$ (**1**), leads to the selective coordination of [*cis*,*cis*,*cis*-$RuCl_2(Me_2SO)_2(CO)$] fragments ([**Ru**]) to some of the peripheral 4′-N sites of the 4′-PyPs. Column separation afforded four partially ruthenated 4′-PyPs in pure form: 4′-*cis*-DPyP[**Ru**] (**2**), 4′-*trans*-DPyP[**Ru**] (**3**), (4′-TPyP)[**Ru**] (**4**), and (4′-TPyP)[**Ru**]$_3$ (**5**). These compounds, which have residual unbound peripheral 4′-N(py) sites (either one or three), were allowed to react with other metal centers that may belong either to a metalloporphyrin or to a coordination compound. When building blocks **2**−**5** were treated with [Ru(TPP)(CO)(EtOH)] (TPP = *meso*-tetraphenylporphyrin) in chloroform at room temperature, axial coordination of Ru(TPP)(CO) units ((**Ru**)) to the available 4′-N(py) sites readily occurred, generating the following arrays containing both perpendicular porphyrins and coordination compounds: (**Ru**)-(μ-4′-*cis*-DPyP)[**Ru**], (**Ru**)(μ-4′-*trans*-DPyP)[**Ru**], (**Ru**)$_3$(μ-4′-TPyP)[**Ru**], and (**Ru**)(μ-4′-TPyP)[**Ru**]$_3$. Furthermore, building blocks **2**, **3**, and **5** were treated with a series of coordination compounds capable of binding two pyridylporphyrins either cis to each other (*trans*-$RuCl_2(Me_2SO)_4$ and *trans*,*cis*,*cis*-$RuCl_2(Me_2SO)_2(CO)_2$) or trans to each other (*trans*-$PdCl_2(C_6H_5CN)_2$). Homo- (Ru) and heterobimetallic (Ru−Pd) arrays with as many as seven metal atoms (six Ru and one Pd) and two 4′-PyPs were obtained as follows: *trans*,*cis*,*cis*-$RuCl_2(Me_2SO)_2$(4′-*cis*-DPyP[**Ru**])$_2$, *trans*,*cis*,*cis*-$RuCl_2(Me_2SO)_2$(4′-*trans*-DPyP[**Ru**])$_2$, *trans*,*cis*,*cis*-$RuCl_2(CO)_2$(4′-*cis*-DPyP[**Ru**])$_2$, and *trans*-$PdCl_2$(4′-TPyP[**Ru**]$_3$)$_2$. All the products were thoroughly characterized by ^{1}H NMR spectroscopy. Since the [**Ru**] fragment is chiral, diastereomers are formed when two or more [**Ru**] units are bound to a porphyrin. We found that when two 4′-*cis*-DPyP[**Ru**] (**2**) units are coordinated cis to each other on the same metal center, the mutual anisotropic effect of the cis porphyrins differentiates the sulfoxide methyl resonances for the two forms. These and other results indicate that the pyridyl units react independently of the presence or absence of a substituent on the other py rings. Thus, the synthetic strategy should be a general method for linking diverse metal centers through pyridylporphyrins.

Introduction

The coordination bond motif, as an alternative to covalent bond formation, is being increasingly exploited for the construction of supramolecular arrays.[1] The inclusion of porphyrins and metalloporphyrins into supramolecular systems is of prime interest because of their inherent useful photochemical and redox properties. In particular, arrays of porphyrins are being investigated as models of the photosynthetic system and as potential light-harvesting devices.[2,3]

Building block methodologies utilizing metal-mediated supramolecular self-assembly provide an attractive alternative approach for construction of large arrays of covalently linked macrocycles.[3c,4] One such approach exploits the formation of coordination bonds between a peripheral basic site(s) on the porphyrins and metal centers, which may belong either to a metalloporphyrin or to a coordination complex.[5]

Within this frame, *meso*-pyridyl/phenyl porphyrins (PyPs)[6] proved to be particularly versatile building blocks: PyPs can provide geometrically well-defined connections to as many as four metal centers by coordination of the pyridyl groups (Chart

* To whom correspondence should be addressed. Fax: +39 040 6763903. E-mail: alessi@univ.trieste.it.

† Università di Trieste.

‡ On leave from Department of Chemistry, St. Petersburg State University, 198904 Stary Petergof, Russian Federation.

§ Emory University.

(1) (a) Stang, P. J. *Chem. Eur. J.* **1998**, *4*, 19−27. (b) Fujita, M. *Chem. Soc. Rev.* **1998**, *27*, 417−425. (c) Olenyuk, B.; Fechtenkötter, A.; Stang, P. J. *J. Chem. Soc., Dalton Trans.* **1998**, 1707−1728. (d) Jones, C. J. *Chem. Soc. Rev.* **1998**, *27*, 289−299. (e) Stang, P. J.; Olenyuk, B. *Acc. Chem. Res.* **1997**, *30*, 502−518.

(2) (a) Harriman, A.; Sauvage, J.-P. *Chem. Soc. Rev.* **1996**, 41−48. (b) Kurreck, H.; Huber, M. *Angew. Chem., Int. Ed. Engl.* **1995**, *34*, 849−866. (c) Lin, V. S.-Y.; DiMagno, S. G.; Therien, M. J. *Science* **1994**, *264*, 1105−1111. (d) Wasielewski, M. R. *Chem. Rev.* **1992**, *92*, 435−461.

(3) (a) Prodi, A.; Indelli, M. T.; Kleverlaan, C. J.; Scandola, F.; Alessio, E.; Gianferrara, T.; Marzilli, L. G. *Chem. Eur. J.* **1999**, *5*, 2668. (b) Wagner, R. W.; Seth, J.; Yang, S. I.; Kim, D.; Bocian, D. F.; Holten, D.; Lindsey, J. S. *J. Org. Chem.* **1998**, *63*, 5042−5049 and references therein. (c) Nakano, A.; Osuka, A.; Yamazaki, I.; Yamazaki, T.; Nishimura, Y. *Angew. Chem., Int. Ed. Engl.* **1998**, *37*, 3023−3027. (d) Seth, J.; Palaniappan, V.; Johnson, T. E.; Prathapan, S.; Lindsey, J. S.; Bocian, D. F. *J. Am. Chem. Soc.* **1994**, *116*, 10578−10592.

(4) (a) Mak, C. C.; Bampos, N.; Sanders, J. K. M. *Angew. Chem., Int. Ed. Engl.* **1998**, *37*, 3020−3022. (b) Officer, D. L.; Burrell, A. K.; Reid, D. C. W. *Chem. Commun.* **1996**, 1657−1658 and references therein.

10.1021/ic990709a CCC: $19.00
Published on Web 03/04/2000

Chart 1. *meso*-4′-Pyridylporphyrins Used in This Work Together with Their Schematic Building Block Representation

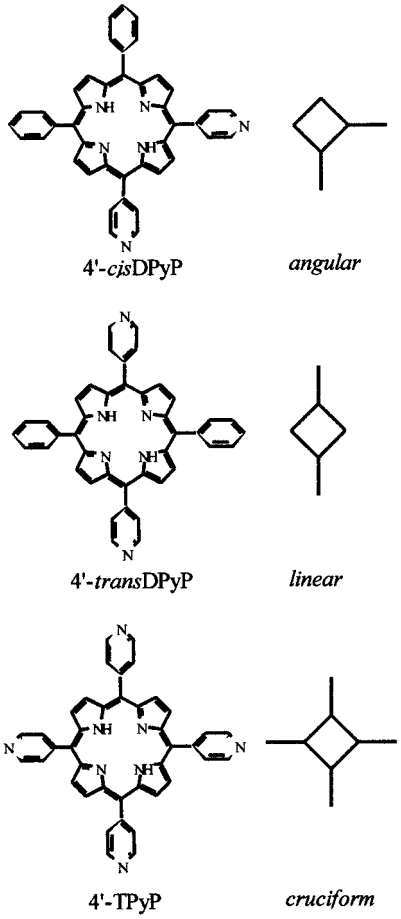

1). The peripheral N atom can be either in the 4′ (4′-PyPs), in the 3′ (3′-PyPs), or in the 2′ (2′-PyPs) position. Coordination of the 4′-N(py) groups of *meso*-pyridylporphyrins to ruthenium,[7,8] osmium,[9] zinc,[10] and manganese porphyrins[11] with substitutionally labile axial ligands leads either to discrete arrays or to polymers and networks of perpendicular axially ligated porphyrins, depending on the choice of the building blocks. Canted analogues were obtained using 3′-PyPs instead of 4′-PyPs.[7a,b,9a] Moreover, metallo-PyPs can self-assemble in solution into linear[12] or cyclic oligomers,[13] including cofacial systems when the N atom is in the 2′ position.[14]

Several discrete supramolecular assemblies, derived by ligation of 4′-PyPs to coordination compounds have been reported;[15,16] depending on the nature of the metal center(s) and of the 4′-PyP linker(s), these assemblies exhibit a rather wide range of nuclearities, both in term of metals and in terms of porphyrin units. Moreover, 4′-PyPs or closely related pyridylporphyrins have also been employed as linear or angular building blocks for the construction of molecular squares.[17] To date, the most striking result of this powerful synthetic methodology is the discrete nonameric array described by Drain, involving coordination of three different types of 4′-PyPs to 12 palladium(II) units.[18]

However, to our knowledge, in all the adducts reported to date the central PyP unit is symmetrically substituted; i.e., all the peripheral pyridyl nitrogen atoms are linked to metal centers with the same coordination environment. The importance of establishing a synthetic approach toward unsymmetrical adducts is readily understood; for example, a proper choice of the metal components bound to the central pyridylporphyrin might favor electron and/or charge transfer from one site to another within the unsymmetrical supramolecular adduct.

We describe here the stepwise coordination of 4′-PyPs to diverse metal centers, leading to the construction of unprecedented unsymmetrical discrete arrays containing porphyrins and coordination complexes.

Experimental Section

General Methods. Hydrated $RuCl_3$ was a loan from Johnson Matthey. *cis,fac*-$RuCl_2(Me_2SO)_3(CO)$,[19] *trans*-$RuCl_2(Me_2SO)_4$,[20] *trans*,-

(5) (a) Burrell, A. K.; Officer, D. L.; Reid, D. C. W.; Wild, K. Y. *Angew. Chem., Int. Ed. Engl.* **1998**, *37*, 114−117. (b) Krishna Kumar, R.; Balasubramanian, S.; Goldberg, I. *Inorg. Chem.* **1998**, *37*, 541−552. (c) Kuroda, Y.; Kato, Y.; Ogoshi, H. *Chem. Commun.* **1997**, 469−470. (d) Stibrany, R. T.; Vasudevan, J.; Knapp, S.; Potenza, J. A.; Emge, T.; Schugar, H. J. *J. Am. Chem. Soc.* **1996**, *118*, 3980−3981. (e) Sarson, L. D.; Ueda, K.; Takeuchi, M.; Shinkai, S. *Chem. Commun.* **1996**, 619−620. (f) Collin, J.-P.; Harriman, A.; Heitz, V.; Odobel, F.; Sauvage, J.-P. *Coord. Chem. Rev.* **1996**, *148*, 63−69. (g) Hunter, C. A.; Hyde, R. K. *Angew. Chem., Int. Ed. Engl.* **1996**, *35*, 1936−1939. (h) Amabilino, D. B.; Dietrich-Buchecker, O.; Sauvage, J.-P. *J. Am. Chem. Soc.* **1996**, *118*, 3285−3286. (i) Kobuke, Y.; Miyaji, H. *Bull. Chem. Soc. Jpn.* **1996**, *69*, 3563−3569. (j) Chi, X.; Guerin, A. J.; Haycock, R. A.; Hunter, C. A.; Sarson L. D. *J. Chem. Soc., Chem. Commun.* **1995**, 2567−2569. (k) Rao, T. A.; Maiya, B. G. *J. Chem. Soc., Chem. Commun.* **1995**, 939−940. (l) Hunter, C. A.; Sarson, L. D. *Angew. Chem., Int. Ed. Engl.* **1994**, *33*, 2313−2316.

(6) Abbreviations: 5-(4′-pyridyl)-10,15,20-triphenylporphyrin (4′-MPyP); 5,10-bis(4′-pyridyl)-15, 20-diphenylporphyrin (4′-*cis*-DPyP); 5,15-bis-(4′-pyridyl)-10,20-diphenylporphyrin (4′-*trans*-DPyP); 5,10,15,20-tetra-(4′-pyridyl)porphyrin (4′-TPyP); tetraphenylporphyrin (TPP); octaethylporphyrin (OEP).

(7) (a) Alessio, E.; Geremia, S.; Mestroni, S.; Iengo, E.; Srnova, I.; Slouf, M. *Inorg. Chem.* **1999**, *38*, 869−875. (b) Alessio, E.; Geremia, S.; Mestroni, S.; Srnova, I.; Slouf, M.; Gianferrara, T.; Prodi, A. *Inorg. Chem.* **1999**, *38*, 2527−2529. (c) Alessio, E.; Macchi, M.; Heath, S.; Marzilli, L. G. *Chem. Commun.* **1996**, 1411−1412.

(8) (a) Funatsu, K.; Kimura, A.; Imamura, T.; Ichimura, A.; Sasaki, Y. *Inorg. Chem.* **1997**, *36*, 1625−1635. (b) Kimura, A.; Funatsu, K.; Imamura, T.; Kido, H.; Sasaki, Y. *Chem. Lett.* **1995**, 207−208.

(9) (a) Kariya, N.; Imamura, T.; Sasaki, Y. *Inorg. Chem.* **1998**, *37*, 1658−1660. (b) Kariya, N.; Imamura, T.; Sasaki, Y. *Inorg. Chem.* **1997**, *36*, 833−839.

(10) (a) Li, M.; Xu, Z.; You, X.; Huang, X.; Zheng, X.; Wang, H. *Inorg. Chim. Acta* **1997**, *261*, 211−215. (b) Chernook, A. V.; Rempel, U.; von Borczyskowski, C.; Shugla, A. M.; Zenkevich, E. I. *Chem. Phys. Lett.* **1996**, *254*, 229−241. (c) Anderson, S.; Anderson, H. L.; Bashall, A.; McPartlin, M.; Sanders, J. K. M. *Angew. Chem., Int. Ed. Engl.* **1995**, *34*, 1096−1099.

(11) Krishna Kumar, R.; Goldberg, I. *Angew. Chem., Int. Ed. Engl.* **1998**, *37*, 3027−3030.

(12) Fleischer, E. B.; Shachter, A. M. *Inorg. Chem.* **1991**, *30*, 3763−3769.

(13) (a) Funatsu, K.; Imamura, T.; Ichimura, A.; Sasaki, Y. *Inorg. Chem.* **1998**, *37*, 1798−1804. (b) Funatsu, K.; Kimura, A.; Imamura, T.; Sasaki, Y. *Chem. Lett.* **1995**, 765−766.

(14) (a) Gerasimchuk, N. N.; Mokhir, A. A.; Rodgers, K. R. *Inorg. Chem.* **1998**, *37*, 5641−5650. (b) Funatsu, K.; Imamura, T.; Ichimura, A.; Sasaki, Y. *Inorg. Chem.* **1998**, *37*, 4986−4995.

(15) Alessio, E.; Macchi, M.; Heath, S. L.; Marzilli L. G. *Inorg. Chem.* **1997**, *36*, 5614−5623.

(16) (a) Yuan, H.; Thomas, L.; Woo, L. K. *Inorg. Chem.* **1996**, *35*, 2808−2817. (b) Araki, K.; Toma, H. E. *J. Photochem. Photobiol. A* **1994**, *83*, 245−250. (c) Steiger, B.; Shi, C.; Anson, F. C. *Inorg. Chem.* **1993**, *32*, 2107−2113. (d) Araki, K.; Toma, H. E. *Inorg. Chim. Acta* **1991**, *179*, 293−296.

(17) (a) Fan, J.; Whiteford, J. A.; Olenyuk, B.; Levin, M. D.; Stang, P. J.; Fleisher, E. B. *J. Am. Chem. Soc.* **1999**, *121*, 2741−2752. (b) Stang, P. J.; Fan, J.; Olenyuk, B. *Chem. Commun.* **1997**, 1453−1454. (c) Slone, R. V.; Hupp, J. T. *Inorg. Chem.* **1997**, *36*, 5422−5423. (d) Drain, C. M.; Lehn, J.-M. *J. Chem. Soc. Chem. Commun.* **1994**, 2313−2315. (e) Iengo, E.; Milani, B.; Zangrando, E.; Geremia, S.; Alessio, E. *Angew. Chem., Int. Ed. Engl.*, in press.

(18) Drain, C. M.; Nifiatis, F.; Vasenko, A.; Batteas, J. D. *Angew. Chem., Int. Ed. Engl.* **1998**, *37*, 2344−2347.

(19) Alessio, E.; Milani, B.; Bolle, M.; Mestroni, G.; Faleschini, P.; Todone, F.; Geremia, S.; Calligaris, M. *Inorg. Chem.* **1995**, *34*, 4722−4734.

(20) Alessio, E.; Mestroni, G.; Nardin, G.; Attia, W. M.; Calligaris, M.; Sava, G.; Zorzet, S. *Inorg. Chem.* **1988**, *27*, 4099−4106.

cis,cis-$RuCl_2(Me_2SO)_2(CO)_2$,[19] *trans*-$PdCl_2(C_6H_5CN)_2$,[21] and Ru(TPP)(CO)(EtOH)[22] were prepared according to the literature procedures. Except for 4′-TPyP, which was acquired from Aldrich, the other 4′-PyPs samples were prepared and separated as described.[12,15] All reagents were analytical grade. Column chromatography was performed on 60 Å 230−400 mesh silica gel (Merck). UV−vis spectra were obtained on a Jasco V-550 spectrophotometer. ^{1}H NMR spectra were recorded at 400 MHz on a JEOL EX400 FT instrument. All spectra were run at room temperature in $CDCl_3$ (Aldrich). Proton peak positions are referenced to the peak of residual nondeuterated solvent set at 7.26 ppm, and assignments were made with the aid of 2D correlation spectroscopy (COSY) experiments as detailed below. Solid-state infrared spectra were obtained as Nujol mulls between CsI windows on a Perkin-Elmer 983G spectrometer. Elemental analyses were performed by Dr. E. Cebulec (Dipartimento Scienze Chimiche, Università di Trieste).

4′-*cis*-DPyP[*cis,cis,cis*-$RuCl_2(Me_2SO)_2(CO)$] (2). A mixture of 100 mg of 4′-*cis*-DPyP (0.15 mmol) and 43.4 mg of *cis,fac*-$RuCl_2(Me_2SO)_3(CO)$ (**1**, 0.10 mmol) dissolved in 20 mL of $CHCl_3$ was allowed to react for 3 days at room temperature (in order to minimize the amount of bisruthenated adduct in favor of the reusable unsubstituted porphyrin, 4′-*cis*-DPyP was treated with a substoichiometric amount of **1**). Thin-layer chromatography of the crude product, run in 98% CH_2Cl_2 and 2% EtOH, showed it to be a mixture of three compounds, identified as 4′-*cis*-DPyP[*cis,cis,cis*-$RuCl_2(Me_2SO)_2(CO)]_2$ (R_f = 0.79), 4′-*cis*-DPyP[*cis,cis,cis*-$RuCl_2(Me_2SO)_2(CO)$] (**2**, R_f = 0.67), and 4′-*cis*-DPyP (R_f = 0.64). The products were separated using column chromatography. The column (3.5 cm × 30 cm) was eluted with a CH_2Cl_2/EtOH mixture, gradually changing from the initial 97/3 to a final 95/5 ratio. The desired product was eluted in the central deep-purple band and needed no further purification. Yield: 30 mg, 30%. Anal. Calcd for $C_{47}H_{40}N_6Cl_2O_3RuS_2\cdot0.5\ CHCl_3$ (M_r = 1032.68): C, 54.8; H. 3.9; N, 8.1. Found: C, 55.4; H, 4.1; N, 8.0. UV−vis spectrum [λ, nm ($\epsilon \times 10^4$, $cm^{-1}\ M^{-1}$)] in $CHCl_3$: 420 (38.6), 516 (2.1), 552 (1.0), 591 (0.8), 646 (0.5). Selected IR bands (Nujol, cm^{-1}): $\nu_{C\equiv O}$ = 1978 (vs); $\nu_{S=O}$ = 1112 (s); ν_{Ru-S} = 423 (m).

4′-*trans*-DPyP[*cis,cis,cis*-$RuCl_2(Me_2SO)_2(CO)$] (3). A procedure similar to that described above for **2** was followed. TLC analysis (CH_2Cl_2/EtOH 98/2): 4′-*trans*-DPyP[*cis,cis,cis*-$RuCl_2(Me_2SO)_2(CO)]_2$ (R_f = 0.82), 4′-*trans*-DPyP[*cis,cis,cis*-$RuCl_2(Me_2SO)_2(CO)$] (**3**, R_f = 0.78), and 4′-*trans*-DPyP (R_f = 0.71). After column chromatography of the crude product, pure **3** (11.5 mg, 28% yield), was recovered from reaction of 40 mg of 4′-*trans*-DPyP (0.06 mmol) and 17.4 mg of *cis,fac*-$RuCl_2(Me_2SO)_3(CO)$ (0.04 mmol), originally dissolved in 10 mL of $CHCl_3$. Anal. Calcd for $C_{47}H_{40}N_6Cl_2O_3RuS_2\cdot0.5\ CHCl_3$ (M_r = 1032.68): C, 54.8; H. 3.9; N, 8.1. Found: C, 55.1; H, 4.2; N, 8.0. UV−vis spectrum [λ, nm ($\epsilon \times 10^4$, $cm^{-1}\ M^{-1}$)] in $CHCl_3$: 420 (37.7), 516 (2.0), 552 (1.0), 590 (0.7), 647 (0.5). Selected IR bands (Nujol, cm^{-1}): $\nu_{C\equiv O}$ = 1978 (vs); $\nu_{S=O}$ = 1110 (s); ν_{Ru-S} = 423 (m).

(4′-TPyP)[*cis,cis,cis*-$RuCl_2(Me_2SO)_2(CO)$] (4). A mixture of 200 mg of 4′-TPyP (0.23 mmol) and 140.4 mg of *cis,fac*-$RuCl_2(Me_2SO)_3(CO)$ (**1**, 0.23 mmol) dissolved in 25 mL of $CHCl_3$ was allowed to react for 3 days at room temperature. Thin-layer chromatography of the crude product (CH_2Cl_2/EtOH, 90/10) showed it to be a mixture of six compounds identified as 4′-TPyP[*cis,cis,cis*-$RuCl_2(Me_2SO)_2(CO)]_4$ (R_f = 0.61), 4′-TPyP[*cis,cis,cis*-$RuCl_2(Me_2SO)_2(CO)]_3$ (**5**, R_f = 0.56), *trans*-4′-TPyP[*cis,cis,cis*-$RuCl_2(Me_2SO)_2(CO)]_2$ (R_f = 0.52), *cis*-4′-TPyP[*cis,cis,cis*-$RuCl_2(Me_2SO)_2(CO)]_2$ (R_f = 0.50), 4′-TPyP[*cis,cis,cis*-$RuCl_2(Me_2SO)_2(CO)$] (**4**, R_f = 0.46), and 4′-TPyP (R_f = 0.40). The products were separated using flash column chromatography. The column (3 cm × 15 cm) was eluted with a CH_2Cl_2/EtOH mixture (93/7). Compound **4** was eluted in the fifth band (even though the two bisruthenated isomers are often eluted in a single band). Yield: 70 mg, 25%. Anal. Calcd for $C_{45}H_{38}N_8Cl_2O_3RuS_2\cdot1.5CH_2Cl_2\cdot H_2O$ (M_r = 1120.35): C, 49.8; H, 3.8; N, 10.0. Found: C, 49.8; H, 3.9; N, 9.8. UV−vis spectrum [λ, nm ($\epsilon \times 10^4$, $cm^{-1}\ M^{-1}$)] in $CHCl_3$: 419 (31.3), 514 (1.8), 549 (0.6), 589 (0.6), 645 (0.2). Selected IR bands (Nujol, cm^{-1}): $\nu_{C\equiv O}$ = 1981 (vs); $\nu_{S=O}$ = 1113 (s); ν_{Ru-S} = 424 (m).

(4′-TPyP)[*cis,cis,cis*-$RuCl_2(Me_2SO)_2(CO)]_3$ (5). A procedure similar to that described above for **4** was followed except for the stoichiometric ratio of 4′-TPyP to **1** (1:2 instead of 1:1). Compound **5** was eluted in the second band. Yield: 85 mg, 20%. Anal. Calcd for $C_{55}H_{62}N_8Cl_6O_9Ru_3S_6\cdot2CH_2Cl_2$ (M_r = 1857.29): C, 36.9; H, 3.7; N, 6.0. Found: C, 36.9; H, 3.6; N, 6.1. UV−vis spectrum [λ, nm ($\epsilon \times 10^4$, $cm^{-1}\ M^{-1}$)] in $CHCl_3$: 423 (30.4), 516 (1.8), 551 (0.8), 590 (0.6), 646 (0.3). Selected IR bands (Nujol, cm^{-1}): $\nu_{C\equiv O}$ = 1983 (vs); $\nu_{S=O}$ = 1113 (s); ν_{Ru-S} = 423 (m).

[Ru(TPP)(CO)](*μ*-4′-*cis*-DPyP)[*cis,cis,cis*-$RuCl_2(Me_2SO)_2(CO)$] (6), [Ru(TPP)(CO)](*μ*-4′-*trans*-DPyP)[*cis,cis,cis*-$RuCl_2(Me_2SO)_2(CO)$] (7), $[Ru(TPP)(CO)]_3$(*μ*-4′-TPyP)[*cis,cis,cis*-$RuCl_2(Me_2SO)_2(CO)$] (8), and [Ru(TPP)(CO)](*μ*-4′-TPyP)[*cis,cis,cis*-$RuCl_2(Me_2SO)_2(CO)]_3$ (9). All reactions between the partially ruthenated building blocks **2**−**5** and the stoichiometric amount of [Ru(TPP)(CO)(EtOH)] leading to compounds **6**−**9** were monitored by ^{1}H NMR spectroscopy in deuterated chloroform at room temperature. The reactions were quantitative (by NMR criteria) within 30 min and very selective. Reasonably pure products for NMR purposes (some starting material deriving from an incorrect stoichiometric ratio between the precursors might be present) were obtained by precipitation with *n*-hexane and recrystallization from chloroform/*n*-hexane; however, the products were not pure enough for elemental analysis or quantitative electronic absorption measurements. Attempts to purify further the products by chromatography on silica gel led to their decomposition.

***trans,cis,cis*-$RuCl_2(Me_2SO)_2$(4′-*cis*-DPyP[*cis,cis,cis*-$RuCl_2(Me_2SO)_2(CO)])_2$ (13).** A mixture of 20 mg of 4′-*cis*-DPyP[*cis,cis,cis*-$RuCl_2(Me_2SO)_2(CO)$] (**2**) (0.02 mmol) and 3.8 mg of *trans*-$RuCl_2(Me_2SO)_4$ (**10**, 0.0078 mmol) dissolved in 10 mL of $CHCl_3$ was allowed to react for 24 h at room temperature. Thin-layer chromatography of the crude product, run in 95% CH_2Cl_2 and 5% EtOH, showed it to be a mixture of two main compounds, identified as **2** (R_f = 0.50) and *trans,cis,cis*-$RuCl_2(Me_2SO)_2$(**2**)$_2$ (**13**) (R_f = 0.41). The products were separated using column chromatography. The column (1.5 cm × 10 cm) was eluted with a CH_2Cl_2/EtOH mixture gradually changing from the initial 99/1 to a final 96/4 ratio. The desired product was eluted in the second band. Yield: 12 mg, 70%. The product was sufficiently pure for NMR purposes but not enough for elemental analysis or quantitative electronic absorption measurements.

***trans,cis,cis*-$RuCl_2(Me_2SO)_2$(4′-*trans*-DPyP[*cis,cis,cis*-$RuCl_2(Me_2SO)_2(CO)])_2$ (14).** A procedure similar to that described above for **13** was followed except for the use of 4′-*trans*-DPyP[*cis,cis,cis*-$RuCl_2(Me_2SO)_2(CO)]$ (**3**) instead of 4′-*cis*-DPyP[*cis,cis,cis*-$RuCl_2(Me_2SO)_2(CO)]$ (**2**). Yield: 10 mg, 60%.

***trans,cis,cis*-$RuCl_2(CO)_2$(4′-*cis*-DPyP[*cis,cis,cis*-$RuCl_2(Me_2SO)_2(CO)])_2$ (15).** The reaction between 4′-*cis*-DPyP[*cis,cis,cis*-$RuCl_2(Me_2SO)_2(CO)]$ (**2**) (5 mg, 0.0048 mmol) and *trans,cis,cis*-$RuCl_2(Me_2SO)_2(CO)_2$ (**11**) (1 mg, 0.0024 mmol) was monitored by ^{1}H NMR spectroscopy in $CDCl_3$. The product, *trans,cis,cis*-$RuCl_2(CO)_2$(4′-*cis*-DPyP[*cis,cis,cis*-$RuCl_2(Me_2SO)_2(CO)])_2$ (**15**), was obtained with good selectivity within 10 h at room temperature. Yield (according to NMR integration): 80%.

***trans*-$PdCl_2$(4′-TPyP[*cis,cis,cis*-$RuCl_2(Me_2SO)_2(CO)]_3)_2$ (16).** A mixture of 4 mg of 4′-TPyP[*cis,cis,cis*-$RuCl_2(Me_2SO)_2(CO)]_3$ (**5**) (0.0024 mmol) and 0.4 mg of *trans*-$PdCl_2(C_6H_5CN)_2$ (**12**) (0.001 mmol) dissolved in 5 mL of $CHCl_3$ was allowed to react for 5 h at room temperature. Thin-layer chromatography of the crude product, run in 96% CH_2Cl_2 and 4% EtOH, showed it to be a mixture of two main compounds identified as **5** (R_f = 0.36), and *trans*-$PdCl_2$(4′-TPyP[*cis,cis,cis*-$RuCl_2(Me_2SO)_2(CO)]_3)_2$ (**16**) (R_f = 0.41). The products were separated using preparative TLC (eluent 92/8 CH_2Cl_2/EtOH mixture) and extracted from silica with an acetone/methanol mixture (80/20). Yield: 2.5 mg, 70%. The product was sufficiently pure for NMR purposes.

***trans*-$PdCl_2$(4′-MPyP)$_2$ (17).** A mixture of 120 mg of 4′-MPyP (0.18 mmol) and 30 mg of *trans*-$PdCl_2(C_6H_5CN)_2$ (**12**) (0.078 mmol) dissolved in 15 mL of $CHCl_3$ was allowed to react for 5 h at room temperature. Thin-layer chromatography of the crude product, run in $CHCl_3$, showed it to be a mixture of two main compounds identified

(21) Hartley, F. R. *Organomet. Chem. Rev. A* **1970**, *6*, 119−137.
(22) Collman, J. P.; Barnes, C. E.; Brothers, P. J.; Collins, T. J.; Ozawa, T.; Gallucci, J. C.; Ibers, J. A. *J. Am. Chem. Soc.* **1984**, *106*, 5151−5163.

Chart 2. Schematic Representation of the Four Partially Ruthenated Porphyrinic Building Blocks **2**−**5** with Numbering Scheme; [**Ru**] = [*cis*,*cis*,*cis*-$RuCl_2(Me_2SO)_2$((CO)]

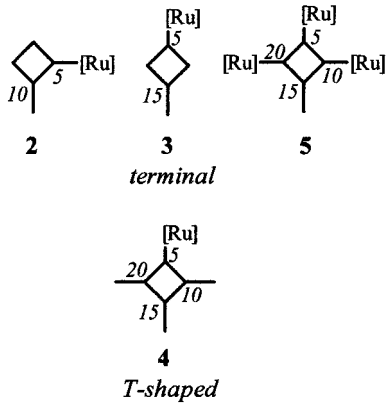

as **17** (R_f = 0.88) and 4′-MPyP (R_f = 0.29). The products were separated using column chromatography. The column (3 cm × 10 cm) was eluted with chloroform. The desired product was eluted in the first band. Yield: 95 mg, 80%. Anal. Calcd for $C_{86}H_{58}N_{10}Cl_2Pd$ (M_r = 1408.77): C, 73.3; H, 4.14; N, 9.94. Found: C, 73.6; H, 4.17; N, 9.85.

Results and Discussion

The *meso*-4′-pyridylporphyrins used in this work are shown in Chart 1, together with their schematic building block representations. Within the frame of the metal-mediated self-assembly, 4′-*cis*-DPyP and 4′-*trans*-DPyP, which bear two peripheral N atoms at 90° and 180°, respectively, may be considered as *angular* and *linear* basic building blocks, respectively. 4′-TPyP has four peripheral N atoms at 90° and is therefore a *cruciform* basic building block.

First Step: Building Blocks. In a synthetic approach involving the stepwise coordination of 4′-PyPs to different metal centers, the metal−4′-N(py) bond(s) formed in the first step must be both stable and inert so that purification of the desired adduct can be performed and scrambling processes in the following step(s) are minimized. For this reason, in the first step we chose 4′-PyPs to react with the Ru(II) complex *cis*,*fac*-$RuCl_2(Me_2SO)_3(CO)$ (**1**). We previously showed that this reaction leads to selective coordination of [*cis*,*cis*,*cis*-$RuCl_2(Me_2SO)_2(CO)$] fragments ([**Ru**]) to the peripheral basic sites of the pyridylporphyrins.[15] In particular, we have described the following fully substituted, stable, inert adducts of 4′-PyPs with **1**: 4′-MPyP-[**Ru**], 4′-*cis*-DPyP[**Ru**]$_2$, 4′-*trans*-DPyP[**Ru**]$_2$, and 4′-TPyP[**Ru**]$_4$. We report now on the synthesis and characterization of 4′-PyPs adducts that are only partially substituted with [**Ru**] units (Chart 2).

Reaction of 4′-*cis*-DPyP with 1 equiv of **1** in chloroform at room temperature yielded, besides unbound porphyrin, a statistical mixture of the known bis-substituted adduct 4′-*cis*-DPyP-[**Ru**]$_2$ and of 4′-*cis*-DPyP[**Ru**] (**2**), where one peripheral 4′-N(py) atom is not coordinated to ruthenium (Figure 1). Column purification of the reaction mixture yielded pure **2**. Similarly, treatment of 4′-*trans*-DPyP with **1** followed by chromatographic separation of the products led to the isolation of 4′-*trans*-DPyP-[**Ru**] (**3**). Finally, two other partially ruthenated porphyrin building blocks were obtained by reaction of 4′-TPyP with **1**. By tuning the 4′-TPyP/**1** ratio, we enriched the mixture of the five possible products (plus unreacted 4′-TPyP) either in the monoruthenated adduct (4′-TPyP)[**Ru**] (**4**), which has three residual peripheral 4′-N(py) sites available for further coordination, or in the trisruthenated product (4′-TPyP)[**Ru**]$_3$ (**5**), which has only one residual peripheral coordination site. Column separation of the mixture afforded pure **4** and **5**.

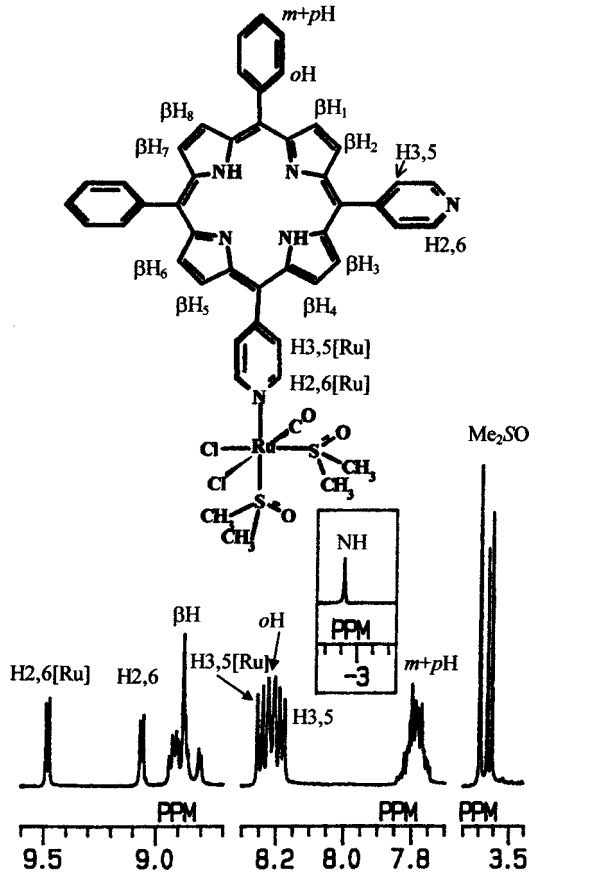

Figure 1. Schematic drawing of 4′-*cis*-DPyP[**Ru**] (**2**) with labeling scheme and its ^{1}H NMR spectrum in $CDCl_3$ (ppm).

The nature and geometry of the purified products was unambiguously established by ^{1}H NMR spectroscopy (Table 1). The NMR characterization of 4′-*cis*-DPyP[*cis*,*cis*,*cis*-$RuCl_2(Me_2SO)_2(CO)$] (**2**) will be described in more detail, since many of the considerations apply also to the other products. In our previous study,[15] we demonstrated that coordination of 4′-PyPs to the [**Ru**] fragment affects mainly the resonances of the pyridyl ring(s) involved in the bond(s), inducing downfield shifts ($\Delta\delta$ H2,6 from 0.3 to 0.9 ppm, $\Delta\delta$ H3,5 from 0.03 to 0.18 ppm).[23] The resonances of the pyrrole protons were particularly informative about the geometry of the adducts, while the Me_2SO signals gave information about the coordination environment of ruthenium. The ^{1}H NMR spectrum of **2** (Figure 1, Table 1), as expected, has two equally intense sets of pyridyl resonances; the most downfield signal (9.47 ppm), attributed to H2,6 of the pyridyl ring bound to [**Ru**], was correlated in the COSY spectrum to the downfield-shifted H3,5 resonance (8.23 ppm). The resonances of H2,6 and H3,5 on the unbound pyridyl ring (position 10), as well as those of the protons on the phenyl rings and of the internal NH's, were not particularly influenced by coordination of [**Ru**]. In accordance with the absence in **2** of mirror planes perpendicular to the porphyrin plane, the eight pyrrole protons are all inequivalent, and their resonances give a complicated pattern of overlapping multiplets. It is well established that in *meso*-pyridylporphyrins rotation about the C(meso)−C(ring) bond is slow on the NMR time scale and that the six-membered rings lie essentially perpendicular to the mean

(23) The chemical shift difference $\Delta\delta$ is defined as δ(adduct) − δ(parent porphyrin).

Table 1. Selected ^{1}H Chemical Shifts of the Partially Ruthenated Building Blocks **2**−**5** in $CDCl_3$ (ppm)

	H2,6−[**Ru**]	H2,6 (py)	Hβ	H3,5−[**Ru**]	H3,5 (py)	Me_2SO	NH
2	9.47 (2,m)[a]	9.06 (2,m)[b]	8.87 (8,m)	8.23 (2,m)[a]	8.16 (2,m)[b]	3.68 (6,s) 3.63 (3,s) 3.60 (3,s)	−2.86 (2,s)
3	9.48 (2,m)[a]	9.05 (2,m)[b]	8.92 (4,m) 8.87 (2,d) 8.81 (2,d)	8.24 (2,m)[a]	8.19 (2,m)[b]	3.69 (6,s) 3.64 (3,s) 3.61 (3,s)	−2.87 (2,s)
4	9.49 (2,m)[a]	9.08 (4,m)[b] 9.07 (2,m)[c]	8.92 (2,d) 8.87 (6,m)	8.22 (2,m)[a]	8.17 (6,m)[b,c]	3.69 (6,s) 3.64 (3,s) 3.63 (3,s)	−2.95 (2,s)
5	9.52 (2,m)[a] 9.50 (4,m)[b]	9.08 (2,m)[c]	8.95 (4,m) 8.91 (2,d) 8.88 (2,d)	8.22 (6,m)[a,b]	8.16 (2,m)[c]	3.69 (9,s) 3.68 (9,s) 3.64 (9,s) 3.62 (9,s)	−2.99 (2,s)

[a] Peaks related to other peaks with superscript "*a*" in the H−H COSY spectrum. [b] Peaks related to other peaks with superscript "*b*" in the H−H COSY spectrum. [c] Peaks related to other peaks with superscript "*c*" in the H−H COSY spectrum.

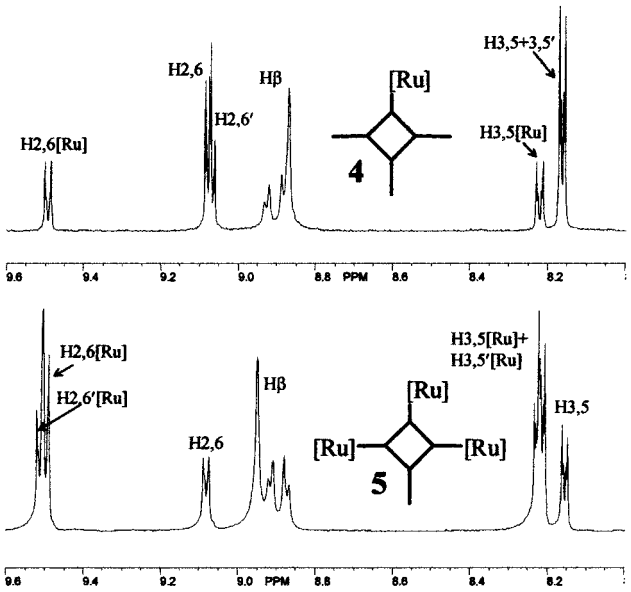

Figure 2. Downfield region of the ^{1}H NMR spectrum of (4′-TPyP)-[**Ru**] (**4**) (top; primed protons belong to the pyridyl ring at position 15) and (4′-TPyP)[**Ru**]$_3$ (**5**) (bottom; primed protons belong to the pyridyl ring at position 5) in $CDCl_3$ (ppm). See Chart 2 for the numbering scheme.

plane of the porphyrin.[7,24] In **2** this plane, despite the presence of the asymmetric [**Ru**] unit, is also a pseudo-mirror plane for the adduct, as demonstrated by the equivalence of protons lying on opposite sites (e.g., H2 and H6). This implies that rotation of the [**Ru**] unit about the 4′-N(py)−Ru bond occurs rapidly on the NMR time scale.

The ^{1}H NMR spectrum of 4′-*trans*-DPyP[**Ru**] (**3**) (Table 1 and Supporting Information) is very similar to that of **2** except for a slight broadening of the H2,6 resonance of the unbound 4′(N)py ring. The resonances of the pyrrole protons reflect the higher symmetry of the adduct, due to the presence of the pseudo-mirror plane perpendicular to the pyridylporphyrin,[25] and consist of four doublets, two of which partially overlap.

The main spectral features of (4′-TPyP)[**Ru**] (**4**) and (4′-TPyP)[**Ru**]$_3$ (**5**) (Figure 2, Table 1) are substantially similar to those for **2** and **3** except for the lack of phenyl resonances; integration established unambiguously in both products the ratio of the pyridyl groups coordinated to [**Ru**] units (with downfield-shifted H2,6 and H3,5 resonances) to the unbound pyridyl groups (with unaffected H2,6 and H3,5 resonances).

In all four building blocks **2**−**5**, the sulfoxide resonances (four equally intense singlets in the region for S-bonded Me_2SO) confirm through integration the number of [**Ru**] fragments bound to each 4′-PyP and are always consistent with the cis,-cis,cis geometry of each ruthenium unit. In the monosubstituted complexes **2**−**4**, however, as already observed in related compounds,[15] the two most downfield methyl resonances may overlap partially or completely. In the trisubstituted adduct **5**, the two sets of Me_2SO resonances in a 1:2 ratio expected for symmetry reasons are not resolved, and four equally intense, slightly broadened, methyl resonances are observed. The broadening of the resonances might be due to the presence of diastereoisomers; in fact, since the [**Ru**] moiety is chiral, **5** must exist as a mixture of stereoisomers (with C or A [**Ru**] units), with potentially different NMR signals. However, at the field used, the ^{1}H NMR signals were not distinct for the diastereoisomers, suggesting that the units are not close enough to have an effect on the shifts.

As found for the fully ruthenated 4′-PyPs previously described by us,[15] the electronic absorption spectra of **2**−**5** are substantially similar to those of the corresponding 4′-PyPs, both in terms of positions and intensities of the Soret and Q bands. In the solid state, the building blocks are characterized by CO stretching frequencies at about 1980 cm^{-1} and by S−O stretching frequencies at about 1100 cm^{-1}, typical for S-bonded Me_2SO.

Second Step: Construction of Unsymmetrical Supramolecular Arrays of Porphyrins. Compounds **2**, **3**, and **5**, having only one residual unbound 4′-N(py) ring, are described as *terminal* basic building blocks. Similarly, compound **4**, which has three residual peripheral 4′-N(py) binding sites at 90° from one another, is described as a *T-shaped* basic building block (Chart 2).

In the second step of our synthetic strategy, this set of four partially ruthenated building blocks was treated with a number of metal centers (acidic building blocks) with the aim of constructing unsymmetrical arrays containing porphyrins and coordination compounds. Examples in which the second metal center lies either inside another porphyrin ring or in a coordination compound will be described.

(a) Reaction of the Building Blocks 2−5 with Metalloporphyrins. We and others have shown that the 4′-N(py) groups of 4′-PyPs bind easily to metalloporphyrins with substitutionally labile axial ligands, such as [Ru(TPP)(CO)(EtOH)] or [Ru(OEP)(CO)(EtOH)],[6] to yield a series of oligomers of perpendicularly linked porphyrins.[7,8] The same procedure was successfully applied here to the partially ruthenated pyridylporphyins

(24) Eaton, S. S.; Eaton, G. R. *J. Am. Chem. Soc.* **1975**, *97*, 3660−3666.
(25) This is a pseudo-mirror plane because at room temperature the rate of the tautomeric NH exchange process is fast on the NMR time scale (see ref 7a).

Chart 3. Schematic Representation of Compounds **6**−**9**[a]

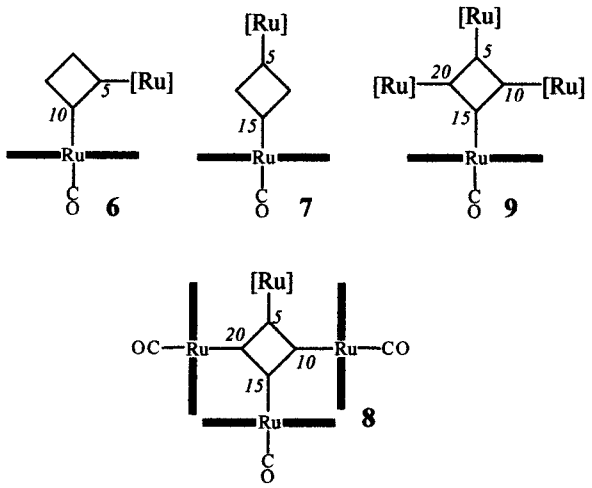

[a] Side-viewed TPP is schematized with a thick line.

2−**5**, which were treated with [Ru(TPP)(CO)(EtOH)] to yield fully substituted 4′-PyPs, in which the previously unbound 4′-N(py) sites are coordinated to Ru(TPP)(CO) unit(s) ((**Ru**), Chart 3). The reactions, followed by ^{1}H NMR spectroscopy ($CDCl_3$, room temperature), were quantitative and selective; chemical shift considerations (Table 2), supported by H−H COSY spectra and integration, allowed us to establish unambiguously the number and site(s) of coordination of Ru(TPP)(CO) unit(s) to the pyridylporphyrins and the geometry of the adducts.

The reaction of 4′-*cis*-DPyP[**Ru**] (**2**) will be described in more detail: coordination of the free 4′-pyridyl group of **2** to [Ru(TPP)(CO)(EtOH)] selectively yielded (**Ru**)(*μ*-4′-*cis*-DPyP)[**Ru**] (**6**) (Chart 3), an adduct of two orthogonal axially ligated porphyrins in which the *cis*-dipyridylporphyrin acts as linker between two different ruthenium centers. Relative to **2**, all resonances of **6** are shifted upfield by the anisotropic shielding cone of the orthogonal ruthenium porphyrin (Table 2, Figure 3). The shielding effect decreases gradually as the (**Ru**)−proton distance increases. Accordingly, the resonances of the protons on the 4′-N(py) ring bound to (**Ru**) are shifted dramatically upfield, especially that of H2,6 ($\Delta\delta = -7.09$ ppm),[23] while those of the protons on the 4′-N(py) ring bound to [**Ru**] are only marginally affected. Moreover, in agreement with the geometry of **6**, coordination of (**Ru**) affects the H3,5 resonance in the cis 4′-N(py)−[**Ru**] ring ($\Delta\delta = -0.22$ ppm) more than that of the corresponding H2,6 ($\Delta\delta = -0.09$ ppm). Also the *o*-protons of the two chemically inequivalent phenyl rings of 4′-*cis*-DPyP give two resolved resonances, both shifted upfield ($\Delta\delta = -0.20$ and -0.13 ppm, respectively) compared to **2**. By analogy with the upfield shift experienced by the H3,5 resonance of 4′-N(py)−[**Ru**], we assigned the most upfield-shifted *o*-H resonance (*o*H^s in Figure 3) to the protons on the phenyl ring at position 15, i.e., cis to 4′-N(py)−(**Ru**).

Because of the absence in **6** of pseudo-mirror planes perpendicular to the pyridylporphyrin, the eight pyrrole protons of 4′-*cis*-DPyP (βH) are all inequivalent; the resonances of βH_2 and βH_3, the protons closest to the ruthenium porphyrin, are shifted upfield to 7.37 and 7.66 ppm, respectively (Figure 3). These two doublets, each integrated for one proton and not connected by a COSY cross-peak, are both correlated to a multiplet at 8.46 ppm, integrated for two protons, attributed to βH_1 and βH_4. The remaining four pyrrole protons on the other side of 4′-*cis*-DPyP with respect to (**Ru**) give a multiplet shifted only slightly upfield to ca. 8.7 ppm and overlapping with the βH resonance of TPP. As established in similar compounds,[7] internal NH resonances are shifted upfield by ca. 0.5 ppm by coordination of the orthogonal (**Ru**).

As was evident for the precursor **2**, in **6** the main plane of 4′-*cis*-DPyP is also a time-averaged mirror plane. Thus, if the six-membered rings of 4′-*cis*-DPyP are assumed to adopt on average a position perpendicular to the mean plane of the porphyrin, both [**Ru**] and (**Ru**) fragments must rotate rapidly enough on the NMR time scale about the 4′-N(py)−Ru bonds to create a mean mirror plane. In accordance with this finding, all four phenyl rings of TPP are equivalent. However, rotation of the phenyl rings about the C(meso)−C(phenyl) bond is slow on the NMR time scale; in fact, the pairs of *o*- and *m*-protons of each ring are clearly nonequivalent (the resonances of *m*- and *p*-protons of TPP overlap with those of the corresponding protons of the phenyl rings of 4′-*cis*-DPyP). The signals of each pair are distinct multiplets with COSY connections relating *o*- and *m*-protons on each side of the ring (Figure 3). In agreement with a perpendicular orientation of the phenyl rings with respect to the Ru(TPP) plane, the shielding effect of 4′-*cis*-DPyP on the phenyl endo protons (bottom inset of Figure 3) is much larger than on the exo protons. Finally, the Me_2SO resonances are almost unaffected by the coordination of (**Ru**) because their positions are quite removed from the shielding cone of TPP.

Treatment of 4′-*trans*-DPyP[**Ru**] (**3**) with [Ru(TPP)(CO)(EtOH)] yielded selectively the corresponding bis(porphyrin) adduct (**Ru**)(*μ*-4′-*trans*-DPyP)[**Ru**] (**7**) (Chart 3). By virtue of the presence of a pseudo-mirror plane perpendicular to 4′-*trans*-DPyP, the ^{1}H NMR spectrum of **7** is simpler than that of the cis isomer **6** (Table 2). The pyrrole resonances (four doublets, two of which partially overlapped with the βH TPP resonance) indicate that in **7** the trans symmetry of the pyridylporphyrin is maintained. Moreover, the two phenyl rings on 4′-*trans*-DPyP are equivalent and only one resonance for the *o*-protons is observed (the resonances of *m*- and *p*-protons of 4′-*trans*-DPyP overlap with those of TPP). The resonances of the 4′-N(py)−[**Ru**] ring are shifted only marginally upfield. In **7** the Me_2SO protons fall into the shielding cone of the ruthenium porphyrin and, even though they are quite far from (**Ru**), their resonances are slightly more upfield-shifted compared to the cis isomer **6**.

Similarly, treatment of (4′-TPyP)[**Ru**] (**4**) and (4′-TPyP)[**Ru**]$_3$ (**5**) with [Ru(TPP)(CO)(EtOH)] yielded (**Ru**)$_3$(*μ*-4′-TPyP)[**Ru**] (**8**) and (**Ru**)(*μ*-4′-TPyP)[**Ru**]$_3$ (**9**), respectively (Chart 3). In both cases the NMR spectrum is consistent with the presence of a pseudo-mirror plane perpendicular to the central 4′-TPyP. In **8**, by virtue of the anisotropy of the cumulative shielding effect of the three ruthenium porphyrins, both the pyridyl (H2,6 and H3,5) and the pyrrole resonances of the two equivalent 4′-N(py)−(**Ru**) moieties trans to each other are well-resolved from those of the 4′-N(py)−(**Ru**) unit trans to [**Ru**] (Table 2). The eight pyrrole protons of 4′-TPyP resonate as four well-resolved doublets, each accounting for 2H; their assignment was made on the basis of chemical shift considerations and of a COSY spectrum (Supporting Information). Also in **9** the anisotropic shielding effect of the (**Ru**) unit allows resolution of some resonances that overlapped in the precursor **5** (Table 2). In fact, the resonance of H3,5 on the two equivalent 4′-N(py)−[**Ru**] rings cis to 4′-N(py)−(**Ru**) is shifted more upfield ($\Delta\delta = -0.22$ ppm) compared to that of the corresponding protons on the 4′-N(py)−[**Ru**] trans to the ruthenium porphyrin ($\Delta\delta = -0.13$ ppm). Moreover, while the 4′-TPyP pyrrole protons lying on the side close to (**Ru**) (βH_1 and βH_2) resonate as two upfield-shifted and well-resolved doublets, the remaining four βH on the other side of 4′-TPyP resonate as an AB multiplet, almost unshifted compared to **5**.

Table 2. Selected ^{1}H Chemical Shifts of Compounds **6**−**9** in $CDCl_3$ (ppm)

	H2,6−[**Ru**]	H2,6−(**Ru**)	Hβ (4′PyP)	Hβ (TPP)	H3,5−[**Ru**]	H3,5−(**Ru**)	*o*-H (PyP)	*o*-H (TPP)	Me_2SO	NH
6	9.39 (2,m)[a]	1.96 (2,m)[b]	8.72 (4,m)[f] 8.46 (2,m)[c,d] 7.37 (1,d)[c] 7.29 (1,d)[d]	8.74 (8,s)[f]	8.02 (2,m)[a]	6.06 (2,m)[b]	8.07 (2,m)[s] 8.00 (2,m)[r]	8.31 (4,m)[eso] 8.19 (4,m)[endo]	3.68 (6,s) 3.64 (3,s) 3.59 (3,s)	−3.32 (2,s)
7	9.39 (2,m)[a]	1.94 (2,m)[b]	8.75 (4,m)[f] 8.47 (2,d)[c] 7.31 (2,d)[c]	8.73 (8,s)[f]	8.17 (2,m)[a]	6.05 (2,m)[b]	7.99 (4,m)	8.31 (4,m)[eso] 8.18 (4,m)[endo]	3.65 (3,s) 3.64 (3,s) 3.60 (3,s) 3.55 (3,s)	−3.33 (2,s)
8	9.25 (2,m)[a]	1.81 (4,m)[b,p] 1.78 (2,m)[c,q]	8.22 (2,d)[d] 7.06 (2,d)[d] 6.86 (2,d)[e] 6.81 (2,d)[e]	8.71 (8,s)[q] 8.69 (16,s)[p]	7.68 (2,m)[a]	5.72 (4,m)[b,p] 5.63 (2,m)[c,q]		8.28 (12, m)[eso] 8.05 (12,m)[endo]	3.66 (3,s) 3.64 (3,s) 3.61 (3,s) 3.58 (3,s)	−4.34 (2,s)
9	9.42 (6,m)[a,b]	1.98 (2,m)[c]	8.80 (4,m) 8.48 (2,d)[d] 7.38 (2,d)[d]	8.75 (8,s)	8.09 (2,m)[a,r] 8.00 (4,m)[b,s]	6.05 (2,m)[c]		8.30 (4,m)[eso] 8.19 (4,m)[endo]	3.69 (18,s) 3.64 (9,s) 3.61 (9,s)	−3.45 (2,s)

[a] Peaks related to other peaks with superscript "*a*" in the H−H COSY spectrum. [b] Peaks related to other peaks with superscript "*b*" in the H−H COSY spectrum. [c] Peaks related to other peaks with superscript "*c*" in the H−H COSY spectrum. [d] Peaks related to other peaks with superscript "*d*" in the H−H COSY spectrum. [e] Peaks related to other peaks with superscript "*e*" in the H−H COSY spectrum. [f] Partially overlapped peaks. [p] Cis to [**Ru**]. [q] Trans to [**Ru**]. [r] Trans to (**Ru**). [s] Cis to (**Ru**).

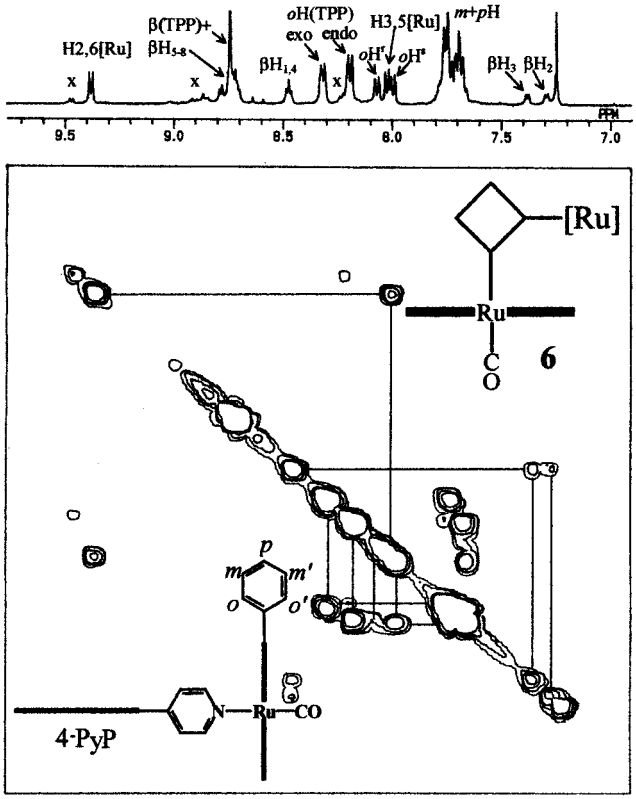

Figure 3. Downfield region of the H−H COSY NMR spectrum of (**Ru**)(μ-4′-*cis*-DPyP)[**Ru**] (**6**) schematically represented at the top. See Chart 3 and Table 2 for the labeling scheme. Peaks marked with x belong to traces of residual **2**. The bottom portion reports a schematic representation of Ru(TPP)(CO) binding to a generic 4′-PyP. All phenyl rings, except the one on TPP, have been omitted for clarity; endo phenyl protons are labeled with *o* and *m*, exo protons with *o*′ and *m*′. The 4′-N(py) and phenyl rings are assumed to lie perpendicularly to the mean plane of 4′-PyP and TPP, respectively. The 4′-N(py)−Ru bond is assumed perpendicular to the TPP plane.

(b) Reaction of the Building Blocks 2−5 with Coordination Compounds. Since the aim of our synthetic strategy is the construction of large molecular arrays, in this step we focused on the reactions of **2**−**5** with coordination compounds that can bind selectively two N ligands either cis or trans to each other. In particular, we used *trans*-$RuCl_2(Me_2SO)_4$ (**10**) and *trans*,*cis*,*cis*-$RuCl_2(Me_2SO)_2(CO)_2$ (**11**) as examples of complexes that can selectively coordinate two building blocks cis to each other,

Chart 4. Schematic Representation of Compounds **13**−**16**[a]

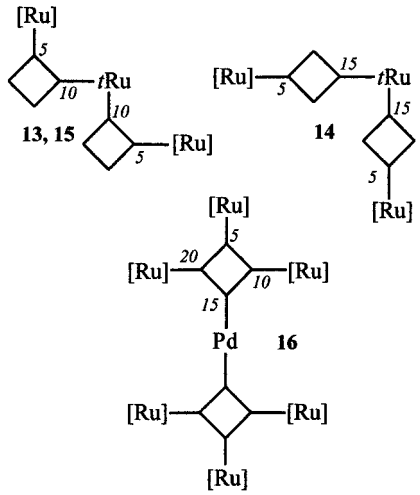

[a] *t***Ru** = *trans*,*cis*-$RuCl_2(X)_2$, X = Me_2SO (**13**, **14**), CO (**15**).

and *trans*-$PdCl_2(C_6H_5CN)_2$ (**12**) as an example for the coordination of two trans building blocks (Chart 4).

In this work, we investigated the reactivity of the ruthenium precursors **10** and **11** with the terminal building blocks 4′-*cis*-DPyP[**Ru**] (**2**) and 4′-*trans*-DPyP[**Ru**] (**3**). Reactions were first monitored by ^{1}H NMR spectroscopy in $CDCl_3$ solution and then, in the case of **2**, performed on a small preparative scale. Compounds **2** and **3** reacted with *trans*-$RuCl_2(Me_2SO)_4$ (2:1 ratio) in much the same way as did 4′-MPyP,[15] leading selectively to the cis-disubstituted products containing three ruthenium centers and two porphyrin rings, *trans*,*cis*,*cis*-$RuCl_2(Me_2SO)_2$(4′-*cis*-DPyP[**Ru**])$_2$ (**13**; Chart 4 and Figure 4) (in shorthand notation *trans*,*cis*,*cis*-$RuCl_2(Me_2SO)_2$(**2**)$_2$) and *trans*,*cis*,*cis*-$RuCl_2(Me_2SO)_2$(4′-*trans*-DPyP[**Ru**])$_2$ (**14**; Chart 4) (in shorthand notation *trans*,*cis*,*cis*-$RuCl_2(Me_2SO)_2$(**3**)$_2$), respectively. Reaction of **2** with *trans*,*cis*,*cis*-$RuCl_2(Me_2SO)_2(CO)_2$ led to *trans*,*cis*,*cis*-$RuCl_2(CO)_2$(4′-*cis*-DPyP[**Ru**])$_2$ (**15**) (in shorthand notation *trans*,*cis*,*cis*-$RuCl_2(CO)_2$(**2**)$_2$). The stoichiometry and the geometry of trimers **13**−**15** were unambiguously established by ^{1}H NMR spectroscopy (Table 3); with the exception of the sulfoxide resonances of **13** (see below), the NMR spectra of **13**−**15** were consistent with a C_{2v} symmetry (the two cis-ruthenated porphyrins are equivalent to each other). Coordination of **2** and **3** to the central *trans*,*cis*-$RuCl_2(X)_2$ moiety (*t***Ru**, X = Me_2SO (**13**, **14**), CO (**15**)) affected mainly

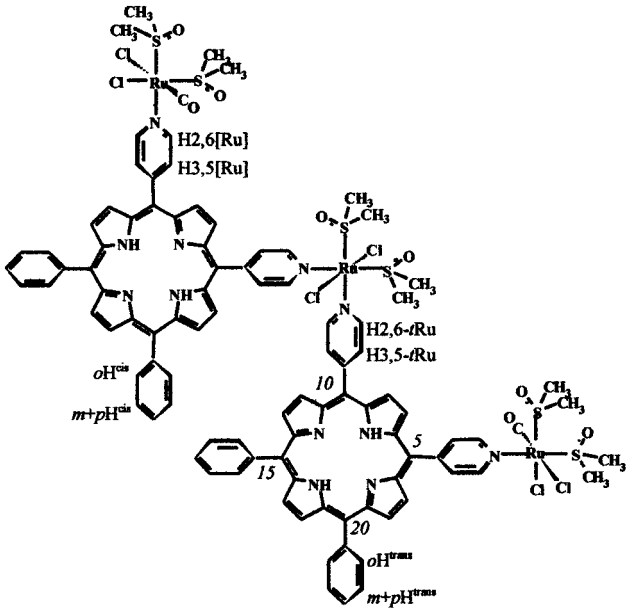

Figure 4. Schematic drawing of *trans,cis,cis*-$RuCl_2(Me_2SO)_2$(4′-*cis*-DPyP[**Ru**])$_2$ (**13**) with labeling scheme.

the H2,6 and H3,5 resonances of the 4′-N(py) ring involved in the new bond, which experienced downfield shifts very similar to those found in the corresponding *trans,cis,cis*-$RuCl_2(X)_2$(4′-MPyP)$_2$ complexes.[15] Conversely, in *trans,cis,cis*-$RuCl_2(Me_2SO)_2$(**2**)$_2$ the resonances of the 4′-(N)py−[**Ru**] ring (position 5) and of the phenyl ring trans to it (position 15) experienced an upfield shift of ca. 0.2 ppm with respect to **2**. Thus, the *o*-H and the (*m* + *p*)-H multiplets of the two cis **2** units are each separated into two equally intense multiplets; the two sets were identified by cross-peaks in the COSY spectrum (Figure 5). This spectral behavior is characteristic of two mutually cis porphyrin units in free rotation about the metal−pyridyl axis; this rotation brings the aromatic rings at the 5,15-positions into the shielding cone of the adjacent porphyrin, as was first reported by us for *trans,cis,cis*-$RuCl_2(Me_2SO)_2$(4′-MPyP)$_2$.[15] The phenyl ring of **2** in position 20 (i.e., trans to the 4′-N(py)−*t***Ru** ring), regardless of the rotation motions of **2**, will never fall into the shielding cone of the adjacent porphyrin, and therefore, its resonances in *trans,cis,cis*-$RuCl_2(Me_2SO)_2$(**2**)$_2$ are substantially unshifted compared to **2**. Similar, although less pronounced, upfield shifts were observed also for *trans,cis,cis*-$RuCl_2(CO)_2$(**2**)$_2$ (**15**) (Table 3). In agreement with these geometrical requirements, in *trans,-cis,cis*-$RuCl_2(Me_2SO)_2$(**3**)$_2$ the resonances of both the equivalent phenyl rings of **3** (positions 10, 20) are shifted upfield, while those of the 4′-N(py)−[**Ru**] ring (position 5) are unshifted compared to **3**.

In the NMR spectrum of *trans,cis,cis*-$RuCl_2(Me_2SO)_2$(**2**)$_2$ (**13**), the very informative region of the sulfoxide resonances deserves a careful examination. First, we notice that the seven resonances (Figure 6) are much more dispersed (between 3.2 and 3.7 ppm) than that usually found in the precursors (in **2** the four methyl groups resonate between 3.60 and 3.68 ppm). The most downfield sharp singlet (3.67 ppm) accounts for 12 protons and was assigned to the two sulfoxide ligands bound on the central *t***Ru** unit for the following reasons: (a) the corresponding resonance falls at 3.65 ppm in *trans,cis,cis*-$RuCl_2(Me_2SO)_2$(4′-MPyP)$_2$;[15] (b) this resonance, unlike the other six more upfield sulfoxide signals, is absent both in the spectrum of the deuterated complex *trans,cis,cis*-$RuCl_2(Me_2SO\text{-}d_6)_2$(**2**)$_2$ [26] and in the spectrum of *trans,cis,cis*-$RuCl_2(CO)_2$(**2**)$_2$ (**15**). Therefore, the remaining six resonances, integrated for 6, 6, 3, 3, 3, 3 protons, respectively, pertain to the four sulfoxides on the two [**Ru**] units. Actually, the most downfield of these six resonances is clearly due to the partial overlap of two equally intense singlets (Figure 6); therefore, we might better consider eight rather than six resonances for the [**Ru**] units, one for each methyl, with two accidental overlaps for the most downfield signals. This number of resonances was unexpected. Thus far, the NMR spectrum of **13** was in agreement with a C_{2v} symmetry for the adduct; the equivalence of the two cis porphyrin units had indicated the existence of a mirror plane containing the two trans chlorides and bisecting the N−Ru−N angle, and the equivalence of the two methyl groups on each sulfoxide ligand on the central *t***Ru** unit also indicates that the N, N, S, S plane is a mirror plane for **13**. From these symmetry considerations four resonances, each accounting for six protons, would be expected for the two equivalent [**Ru**] units in **13**. A saturation transfer experiment allowed us to establish that this higher-than-expected number of sulfoxide resonances is not due to conformational isomers in slow equilibrium on the NMR time scale (saturation of each sulfoxide signal did not involve a decrease in the intensity of any other methyl resonance). They must therefore belong to two equally abundant, not equilibrating, diastereomers.

Indeed, owing to the chirality of the [**Ru**] moiety, the trimeric adduct *trans,cis,cis*-$RuCl_2(Me_2SO)_2$(**2**)$_2$ must exist as an equally abundant mixture of meso (CA, 50%) and racemic (CC + AA, 25 + 25%) forms. Even though, in principle, all resonances might be different in the meso and racemic forms, only those of the [**Ru**] sulfoxides are actually resolved in **13**. In other words, four out of the eight equally intense methyl resonances belong to the 50% meso form of **13**, while the other four belong to the enantiomeric form. We believe that the differentiation of the sulfoxide methyl resonances of [**Ru**] in the two forms of *trans,cis,cis*-$RuCl_2(Me_2SO)_2$(**2**)$_2$ (and of *trans,cis,cis*-$RuCl_2(CO)_2$(**2**)$_2$ as well, Table 3) depends on two factors: (1) the proximity of the [**Ru**] sulfoxide groups to the chiral center; (2) the anisotropic shielding effect of the adjacent porphyrin that, owing to the rotation of **2** about the *t***Ru**−pyridyl axis, induces a differential upfield shift for the [**Ru**] methyl resonances in the meso and racemic forms of **13**, thus allowing their resolution. In other words, the anisotropy of the adjacent porphyrin amplifies the differences in chemical shift for the [**Ru**] methyls in the two diastereomers of **13**. Neither of the two factors alone is sufficient to induce the resolution of methyl sulfoxide signals. For cases in which only factor 1 is present, such as the dimer 4′-*cis*-DPyP[**Ru**]$_2$, the ^{1}H signals of the meso and racemic forms, including those of the sulfoxides, were not distinct.[15] For cases in which only factor 2 is present, for example, the protons of the phenyl ring trans to the 4′-N(py)−[**Ru**] ring, the resonances are shifted upfield, but not differentiated, by the anisotropic effect of the adjacent porphyrin. The combined effect of these two factors is seen also on the 4′-N(py)−[**Ru**] ring H2,6 resonance, which, even though it is not resolved into two distinct signals, is nevertheless broadened (Figure 5). All the other resonances do not give distinct NMR signals because they either are too far from the chiral ruthenium centers or do not fall into the shielding region of the porphyrins.

The spectral features of *trans,cis,cis*-$RuCl_2(Me_2SO)_2$(**3**)$_2$ (**14**) are in good agreement with our interpretation of the NMR spectrum of *trans,cis,cis*-$RuCl_2(Me_2SO)_2$(**2**)$_2$. In fact in **14**, which, as **13**, must exist as an equally abundant mixture of meso and racemic stereomers, the two factors identified above are never encountered together and, at the field used, no ^{1}H NMR

(26) *trans,cis,cis*-$RuCl_2(Me_2SO\text{-}d_6)_2$(**2**)$_2$ was obtained by treatment of *trans*-$RuCl_2(Me_2SO\text{-}d_6)_4$ with **2**, and the reaction was monitored by ^{1}H NMR.

Table 3. Selected ^{1}H Chemical Shifts of Compounds *trans,cis,cis*-$RuCl_2(Me_2SO)_2$(**2**)$_2$ (**13**), *trans,cis,cis*-$RuCl_2(Me_2SO)_2$(**3**)$_2$ (**14**), and *trans,cis,cis*-$RuCl_2(CO)_2$(**2**)$_2$ (**15**) in $CDCl_3$ (ppm)

	H2,6−[**Ru**]	H2,6−*t***Ru**	Hβ	H3,5−[**Ru**]	H3,5−*t***Ru**	*o*-H	(*m* + *p*)-H	Me_2SO	NH
13	9.32 (4,br)[a]	9.85 (4,m)[b]	8.84 (16,m)	8.13 (4,m)[a]	8.33 (4,m)[b]	8.19 (4,m)[c] 8.04 (4,m)[d]	7.79 (6,m)[c] 7.55 (6,m)[d]	3.67 (12,s) 3.57 (6,s) 3.52 (6,s) 3.43 (3,s) 3.41 (3,s) 3.30 (3,s) 3.24 (3,s)	−2.88 (4,s)
14	9.45 (4,m)[a]	9.82 (4,m)[b]	8.86 (16,m)	8.21 (4,m)[a]	8.29 (4,m)[b]	8.04 (4,m)[d]	7.54 (12,m)[d]	3.68 (12,s) 3.65 (12,s) 3.63 (6,s) 3.60 (6,s)	−2.90 (4,s)
15	9.39 (4,br)[a]	9.61 (4,m)[b]	8.86 (16,m)	8.18 (4,m)[a,e]	8.46 (4,m)[b]	8.18 (8,m)[e]	7.79 (6,m)[c] 7.69 (6,m)[d]	3.59 (6,s) 3.54 (6,s) 3.53 (3,s) 3.52 (3,s) 3.44 (3,s) 3.42 (3,s)	−2.85 (4,s)

[a] Peaks related to other peaks with superscript "*a*" in the H−H COSY spectrum. [b] Peaks related to other peaks with superscript "*b*" in the H−H COSY spectrum. [c] Peaks related to other peaks with superscript "*c*" in the H−H COSY spectrum. Phenyl ring in position 15 (trans to *t***Ru**). [d] Peaks related to other peaks with superscript "*d*" in the H−H COSY spectrum. Phenyl ring(s) in position 10 and/or 20 (cis to *t***Ru**). [e] Partially overlapped peaks.

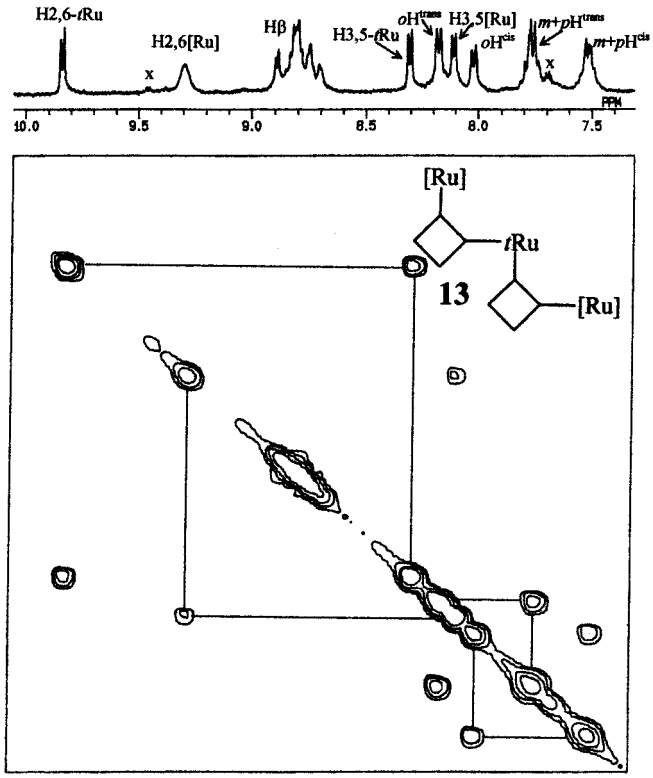

Figure 5. Downfield region of the H−H COSY NMR spectrum of *trans,cis,cis*-$RuCl_2(Me_2SO)_2$(**2**)$_2$ (**13**) schematically represented at the top. See Figure 4 and Table 3 for the labeling scheme. Peaks marked with x belong to traces of residual **2**.

signal was distinct for the two forms. For geometrical reasons, in **14** the [**Ru**] units are not brought into the anisotropic region of the cis porphyrin and only four sulfoxide resonances, spread over a very narrow interval of frequencies, are found (Table 3).

As a final example, we investigated the reaction of (4′-TPyP)-[**Ru**]$_3$ (**5**) with the substitutionally labile square-planar complex bis(benzonitrile)palladium(II) dichloride (2:1 ratio). In chloroform solution at room temperature, two units of **5** replaced the two labile trans benzonitrile ligands readily and selectively (according to ^{1}H NMR spectroscopy) to yield quantitatively

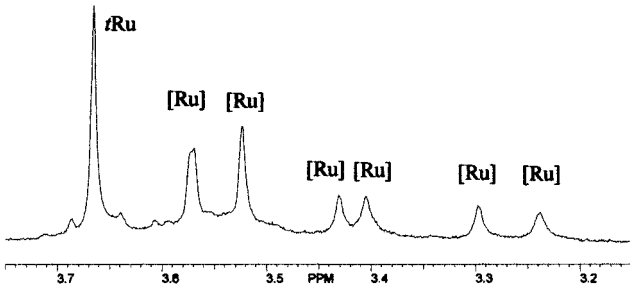

Figure 6. Region of the sulfoxide resonances in the ^{1}H NMR spectrum of *trans,cis,cis*-$RuCl_2(Me_2SO)_2$(**2**)$_2$ (**13**).

trans-$PdCl_2$(4′-TPyP[**Ru**]$_3$)$_2$ (**16**) (in shorthand notation *trans*-$PdCl_2$(**5**)$_2$; (Chart 4). *trans*-$PdCl_2$(**5**)$_2$ is an example of a heterobimetallic supramolecular porphyrin adduct containing two porphyrins and seven metal atoms. The resonances of bound benzonitrile were completely replaced by those of the free ligand, and their integration, compared to that of bound **5**, allowed us to establish unambiguously the stoichiometry of product **16**. Coordination of **5** to Pd induced a downfield shift of the proton resonances in the pyridyl ring involved in the new bond ($\Delta\delta$ H2,6 = 0.4 ppm; $\Delta\delta$ H3,5 = 0.15 ppm), while the other resonances of **5** were only marginally affected (Tables1 and 4). Very similar shifts were observed also in the corresponding complex with monopyridylporphyrin, *trans*-$PdCl_2$(4′-MPyP)$_2$ (**17**), which we prepared for comparative purposes (Table 4). None of the upfield shifts typical of two pyridyl units bound cis to each other on the same metal center were observed in the NMR spectra of **16** and **17**, indicating a trans disposition of the two equivalent pyridyl units in such palladium compounds. Compound **16** contains six chiral ruthenium centers and forms as a complex mixture of diastereoisomers; at the field used, no ^{1}H NMR signal, including the methyl sulfoxide resonances, was distinct for the various forms.

Conclusions

We demonstrated that unsymmetrical arrays containing porphyrins and coordination compounds may be assembled by stepwise coordination of *meso*-4′-pyridylporphyrins (4′-PyPs) to different metal centers.

In the first step, parts of the peripheral basic sites of 4′-PyPs were ligated to the [*cis,cis,cis*-$RuCl_2(Me_2SO)_2(CO)$] fragment

Table 4. ^{1}H Chemical Shifts of Compounds *trans*-$PdCl_2$(**5**)$_2$ (**16**) and *trans*-$PdCl_2$(4′-MPyP)$_2$ (**17**) in $CDCl_3$ (ppm)

	H2,6−[**Ru**]	H2,6−Pd	Hβ	H3,5−[**Ru**]	H3,5−Pd	Me_2SO	NH
16	9.53 (12,m)[a]	9.49 (4,m)[b]	8.97 (16,m)	8.23 (12,m)[a]	8.30 (4,m)[b]	3.70 (31,m) 3.65 (31,m)	−2.98 (4,s)
17		9.41 (4,m)	8.87 (16,m)		8.30 (4,m)		−2.79 (4,s)

[a] Peaks related to other peaks with superscript "*a*" in the H−H COSY spectrum. [b] Peaks related to other peaks with superscript "*b*" in the H−H COSY spectrum.

([**Ru**]); as required in a stepwise synthetic methodology, the 4′-(N)py−[**Ru**] bonds formed in the first step are both stable and inert. Column separation afforded the following four partially ruthenated 4′-PyPs in pure form: 4′-*cis*-DPyP[**Ru**] (**2**), 4′-*trans*-DPyP[**Ru**] (**3**), (4′-TPyP)[**Ru**] (**4**), and (4′-TPyP)[**Ru**]$_3$ (**5**). These compounds, having either one (**2**, **3**, **5**) or three (**4**) residual unbound 4′-(N)py ring(s), may still be considered to be basic building blocks.

In the second step of our synthetic strategy the set of four partially ruthenated porphyrin building blocks **2**−**5** was treated with different metal centers belonging either to metalloporphyrins or to coordination compounds, leading to the final unsymmetrical arrays. Examples of both types were described in detail. In general, we found that coordination of one (or more) [**Ru**] unit(s) to 4′-PyPs did not affect significantly the further reactivity of the uncoordinated 4′-(N)py ring(s). Therefore, we conclude that this work establishes the principle that all pyridyl rings are essentially independent reaction centers.

In the final products the pyridylporphyrins are linkers bridging metalloporphyrins and/or different coordination compounds. These 4′-PyP supramolecular systems are unprecedented, since in all the adducts reported to date the 4′-PyPs were symmetrically substituted; i.e., the peripheral 4′-(N)py sites were bound to metal centers with the same coordination environment. In future, novel unsymmetrical arrays with suitable peripheral metal components, by virtue of the photochemical and redox properties of porphyrins, might favor electron and/or charge transfer from one site to another within the supramolecular adduct.

Acknowledgment. We thank Italian MURST for financial support and Johnson Matthey for a loan of hydrated $RuCl_3$. A 4 month stay of V.Yu.K. in Trieste was supported by a fellowship from Italian National Research Council (C.N.R.).

Supporting Information Available: Schematic drawings of compounds **3**−**9**, **14**, and **16** with labeling schemes, the ^{1}H NMR spectrum of **3**, and the H−H COSY spectrum of **8**. This material is available free of charge via the Internet at http://pubs.acs.org.

IC990709A